# Chiral light-front perturbation theory and the flavor dependence of the light-quark nucleon sea

Mary Alberg [1,2] and Gerald A. Miller [2]
[1] *Department of Physics, Seattle University, Seattle, Washington 98122, USA*
[2] *Department of Physics, University of Washington, Seattle, Washington 98195-1560, USA*

(Received 27 January 2018; revised manuscript received 7 May 2019; published 23 September 2019)

The light-quark flavor dependence of the proton sea has been of great interest for many years because of its close connection with nonperturbative effects. One hypothesis is that this dependence arises from the pion cloud of the proton. We apply light-cone perturbation theory and experimental constraints to a chiral Lagrangian to compute the relevant Fock-space components of the nucleon wave function with well-defined uncertainties. Existing experimental information regarding the light-flavor sea is studied and predictions for future experimental results are provided. Future experiments have the ability to rule out this hypothesis and have profound implications for understanding the nucleon-nucleon force.

DOI: 10.1103/PhysRevC.100.035205

## I. INTRODUCTION

Textbooks tell us that nucleons are composed of $u$ and $d$ valence constituent quarks, but this cannot be the whole story because the gluons inherent in QCD must generate quark-antiquark pairs. Thus one is led to the question: Do the pairs arise only from perturbative evolution at high-momentum scales, or do they have a nonperturbative origin? A definitive answer would provide great help in understanding the nature of confinement and also fundamental aspects of the nucleon-nucleon force. Perturbative QCD predicts a sea that is almost symmetric in light flavor. However, the discovery of the violation of the Gottfried sum rule told us that $\bar{d}$ quarks are favored over $\bar{u}$ quarks [1]. This highlighted the importance of the pion cloud of the nucleon [2,3].

To truly understand the sea one needs to know more. Efforts to measure the ratio $\bar{d}/\bar{u}$ by the E866 collaboration [4,5] have been ongoing and continue with the SeaQuest experiment [6]. Theory is reviewed in Refs. [7,8].

The pionic contribution to the nucleon sea is of special interest. Understanding the pion and its interaction with and among nucleons is a necessary step in learning how QCD describes the existence of atomic nuclei. As a nearly massless excitation of the QCD vacuum, the pion is a harbinger of spontaneous symmetry breaking. The pion is associated with large distance structure of the nucleon [9–11] and its exchange between nucleons provides the longest ranged component of the strong force. The general field of chiral perturbation theory [12,13] is well established.

A nonperturbative sea arises from the pion cloud. We aim to make definitive predictions of the pion-cloud model by providing a light-cone perturbation theory approach capable of making predictions with known uncertainties. Previous calculations have noted ambiguities related to the dependence of the pion-baryon vertex function on momentum transfer and on the possible dependence upon the square of the four-momentum of intermediate baryons, and much discussion has ensued [7,14–24].

There is a vast, deep, and venerated literature on the role of the pion cloud in nucleon structure. Nevertheless, there is still much to be done. For example, even the very first example [2,3], the size of the pion contribution to the $\bar{d}$-$\bar{u}$ asymmetry, is under present controversy. References [18,22] argue that the pion cloud accounts completely for the measured asymmetry. In contrast, Ref. [16] finds that only about half of the asymmetry can be accounted for by pion-cloud effects. In their view, cancellations between the effects of $N$ and $\Delta$ intermediate states, which would be complete in the limit of large $N_c$, reduce the size of the effect. This discrepancy needs to be resolved.

There is another more fundamental issue involving the loss of relativistic invariance which occurs when the vertex function is treated (universally in all of the models so far) as depending on only three of the four necessary momentum variables. This paper resolves both of these problems by using a four-dimensional formalism and by using experimental constraints on the pion-baryon vertex function. The formalism employed here combines pion-baryon dynamics with light-front perturbation theory. Hence the new nomenclature, "chiral light-front perturbation theory" that appears in the title.

## II. FORMALISM

In a light-cone perturbation theory (LCPT) description, the proton wave function can be expressed as a sum of Fock-state components [25–28]. Our hypothesis is that the nonperturbative light-flavor sea originates from the bare nucleon, pion-nucleon ($\pi N$), and pion-Delta ($\pi\Delta$) components. The interactions are described by using the relativistic leading-order chiral Lagrangian [29–31]. Displaying the interaction terms to the relevant order in powers of the pion field, we use

$$\mathcal{L}_{\rm int} = -\frac{g_A}{2f_\pi}\bar{\psi}\gamma_\mu\gamma_5\tau^a\psi\,\partial_\mu\pi^a - \frac{1}{f_\pi^2}\bar{\psi}\gamma_\mu\tau^a\psi\,\epsilon^{abc}\pi^b\partial_\mu\pi^c - \frac{g_{\pi N\Delta}}{2M}\left(\bar{\Delta}^i_\mu g^{\mu\nu}\psi\partial_\nu\pi^i + \text{H.c.}\right), \quad (1)$$

where $\psi$ is the Dirac field of the nucleon, $\pi^a (a = 1, 2, 3)$ is the chiral pion field, and $M$ is the nucleon mass. In Eq. (1), $g_A$

 ©2019 American Physical Society

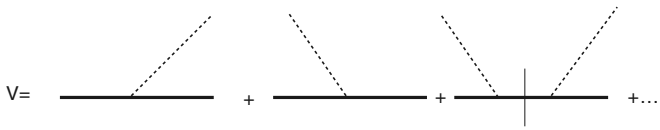


FIG. 1. Terms in the light-front Hamiltonian.

denotes the nucleon axial-vector coupling and $f_\pi$ is the pion-decay constant. The second term is the Weinberg-Tomazowa term which describes low-energy $\pi$-nucleon scattering. In the third term, $g_{\pi N\Delta}$ is the $\pi N\Delta$ coupling constant, and the $\Delta^i_\mu$ field is a vector in both spin and isospin space.

Previous work [32] included the effects of the $\omega$ meson, based on one-boson exchange models of the $NN$ potential. Current treatments do not include the explicit effects of exchanged vector mesons because their masses represent a high-energy scale [33–35]. When computing spin-independent quantities, the small expected effects of such heavy mesons cannot be distinguished from the bare sea of the nucleon. The influence of heavy mesons may be important for spin-dependent effects (see the review [8]), and that topic will be discussed in a later presentation.

The procedure for deriving the LCPT for any Lagrangian is to construct the Hamiltonian operator from the $T^{+-}$ component of the energy-momentum tensor [25,26,28,36,37]. The Hamiltonian can be written in terms of a sum of kinetic-energy operators, $M_0^2$, and interaction terms, denoted as $V$; see Fig. 1. The first two terms are standard interactions, and the third is an instantaneous term that enters only at higher orders in the coupling constant. The Hamiltonian forms of the single-pion emission or absorption terms (Fig. 1) are expressed as matrix elements evaluated between on-shell free nucleon spinors [25,26,28,36,37]. The light-front Schrödinger equation for the proton $p$ is given by $(M_0^2 + V)|p\rangle = M_p^2|p\rangle$. To the desired second-order,

$$|p\rangle \approx \sqrt{Z}|p\rangle_0 + \frac{1}{M_p^2 - M_0^2} V|p\rangle_0, \tag{2}$$

where $|p\rangle_0$ represents the nucleon in the absence of the pion cloud, the bare nucleon, and $Z$ is a normalization constant. This expression is of first order in $V$, hence the term "perturbative." The model is based on the assumption that including higher-order terms is not necessary because including higher-order diagrams would introduce large uncertainties. However, as explained below, the consistency of this approach is maintained by using soft-form vertex functions. Given Eq. (2), the wave function can be expressed as a sum of Fock-space components given by

$$|p\rangle = \sqrt{Z}|p\rangle_0 + \sum_{B=N,\Delta} \int d\Omega_{\pi B} |\pi B\rangle\langle \pi B|p\rangle_0, \tag{3}$$

where $\int d\Omega_{\pi B}$ is a phase-space integral [27,28]. In this formalism the pion momentum distributions $f_{\pi B}(y)$, which represent the probability that a nucleon will fluctuate into a pion of light-front momentum fraction $y$ and a baryon of light-front momentum fraction $1-y$, are squares of wave functions, $|\langle \pi B|\Psi\rangle|^2$, integrated over $k_\perp$.

The Lagrangian of Eq. (1) is incomplete because it is not renormalizable. We tame divergences by using a physically motivated set of regulators, depending on four-momenta, that are constrained by data. If chiral symmetry is maintained, one finds that the $\pi N$ vertex function $g_{\pi N}(t)$ and the nucleon axial form factor are related by the generalized Goldberger-Treiman relation [38] (obtained with $m_\pi = 0$):

$$M g_A(t) = f_\pi g_{\pi N}(t), \tag{4}$$

$$g_A(t) = g_A(0)/\left[1 + \left(t/M_A^2\right)\right]^2, \tag{5}$$

where $t$ is the square of the four-momentum transferred to the nucleon. Equation (4) follows from partial conservation of the axial-vector current (PCAC) and the pion pole dominance of the pseudoscalar current and is obtained from a matrix element of the axial-vector current between two on-mass-shell nucleons. The $t$ dependence of $g_A$ is determined for $t > 0$ by low-momentum-transfer experiments [38], with $M_A$ being the single parameter. Equation (4) relates an essentially unmeasurable quantity $g_{\pi N}(t)$ with one $g_A(t)$ that is constrained by experiments. The major uncertainty in previous calculations is largely removed. Some models (see, e.g., Ref. [39]) find differences between the $t$ dependence of $g_A(t)$ and $g_{\pi N}(t)$, which is allowed because $m_\pi \neq 0$. Uncertainties in the parameter $M_A$ are discussed below, where it is also shown that very large values of $t$ are not important in the calculations of this paper.

In evaluating the nucleon wave function (3), the necessary vertex function must be applicable to situations when either pion or baryon or both are off their mass shells. We use frame-independent pion-baryon form factors, in which a nucleon of mass $M$ and momentum $p$ emits a pion of mass $\mu$ and momentum $k$ and becomes a baryon of mass $M_B$ and momentum $p-k$:

$$F(k,p,y) = \frac{\Lambda^2}{k^2 - \mu^2 - \Lambda^2 + i\epsilon} \frac{\Lambda^2}{\frac{y}{1-y}\left[(p-k)^2 - M_B^2\right] - \Lambda^2 + i\epsilon}. \tag{6}$$

Using $F(k,p,y)$ allows us to obtain a pion-baryon light-front wave function. We explain for the $\pi N$ system. The form factor is part of a model for the $\pi N$ vertex function $\Gamma_a(k,p) = \not{k}\gamma^5 \frac{g_A}{2f_\pi}\tau_a F(k,p,y)$, where $k$ is the pion momentum and $p$ is the nucleon momentum. The $\pi N$ component of the light-front wave function is obtained from the Bethe-Salpeter wave function $\Psi^a_{\pi N}(k,p)$ by integrating over $k^-$ [25,40,41] and projecting onto on-mass-shell baryon spinors:

$$\Psi_{a\mathrm{LF}}(k,p,s) = \frac{M^2 y(1-y)}{2\pi p^+} \int_{-\infty}^{\infty} dk^- \Psi^a_{\pi N}(k,p,s),$$

with $\Psi_{a\mathrm{LF}}(k,p,s) \equiv \langle k,p,s|\pi N\rangle$ and

$$\Psi^a_{\pi N}(k,p,s) = -i\bar{u}(p-k,s)\not{k}\gamma^5 u(p,s)\frac{g_A}{2f_\pi}\tau_a \times \frac{1}{(k^2 - \mu^2 + i\epsilon)[(p-k)^2 - M^2 + i\epsilon]} F(k,p,y). \tag{7}$$

The definition of the light-front wave function uses the basis that the Dirac spinors are evaluated for on-shell kinematics with $(p-k)^- = [(p-k)_\perp^2 + M^2]/(p-k)^+$, so that the numerator factor does not depend on $k^-$, and the integration over $k^-$ involves only the denominator. The evaluation of $\Psi_{a\mathrm{LF}}(k,p,s)$ by integrating over the upper-half $k^-$ plane gives the same result as integration over the lower half. Thus, the light-cone wave function (including the effect of form factors) is uniquely defined. Both procedures yield

$$\Psi_{\mathrm{a,LF}}(k,p,s) = \frac{Mg_A}{2f_\pi(2\pi)^{3/2}}\sqrt{\frac{y}{1-y}}\frac{\bar{u}(p-k)i\gamma^5\tau_a u(p)}{t+\mu^2}F_A(t),$$
$$F_A(t) \equiv \frac{2\Lambda^4}{(\Lambda^2+t+\mu^2)(2\Lambda^2+t+\mu^2)}. \tag{8}$$

Expanding $F_A(t)$ to first order in $t$, comparing the result to the same expansion of $g_A(t)/g_A(0)$, and matching the results determine the value $\Lambda = \sqrt{3}/2M_A$. Numerical results (see below) show that using this $F(k,p,y)$ is equivalent to using a form factor of the form of Eq. (4) in computing $f_{\pi N}(y)$. The parameter independence of this approach is maintained.

The pion two-dimensional momentum distribution function $f_{\pi N}(y,t)$ is obtained by squaring $|\Psi_{\mathrm{a,LF}}(k,p,s)|$ and summing over $a, s$. The result is

$$f_{\pi N}(y,t) = \frac{3M^2}{16\pi^2}\frac{g_A^2}{f_\pi^2}y\frac{t}{(t+\mu^2)^2}F_A^2(t), \tag{9}$$

with $t = (M^2y^2 + k_\perp^2)/(1-y)$. The pion longitudinal momentum distribution function $f_{\pi N}(y)$ is then

$$f_{\pi N}(y) = \int_{t_N}^{\infty} dt\, f_{\pi N}(y,t), \tag{10}$$

where $t_N \equiv M^2y^2/(1-y)$. Using Eq. (4) or (8) yields the same $f_{\pi N}$ because the integrand is dominated by the region of low values of $t$.

It is necessary to show that the pionic effects are of long range when the stated vertex function is used. The formal way to do that is to study the resulting three-dimensional, light-front structure of the pion-baryon component. Here the transverse spatial probability density of the $\pi N$ fluctuation, $\rho_{\pi N}(y,b) = |\psi_{\pi N}(y,b)|^2$, with

$$\psi_{\pi N}(y,b) = \frac{1}{(2\pi)^2}\int_0^\infty d^2\vec{k}_\perp e^{i\vec{k}_\perp\cdot\vec{b}}\Psi_{\mathrm{a,LF}}(k,p), \tag{11}$$

with $k_\perp = [(1-y)t - y^2M^2]^{1/2}$. This distribution represents the spatial extent of the pion cloud but, as pointed out by Burkardt [42], there is no direct connection between transverse momentum space densities $f_{\pi N}(y,k_\perp)$ and transverse position space densities $\rho_{\pi N}(y,b)$.

Next is the intermediate $\Delta$ contribution. The pionic coupling between nucleons and $\Delta$ particles has an off-diagonal Goldberger-Treiman relation [30,43] similar to Eq. (4). Lattice calculations [43] show that $\frac{g_{\pi N\Delta}(t)}{g_{\pi N}(t)} = 1.61$ is constant and consistent with the Goldberger-Treiman relations.

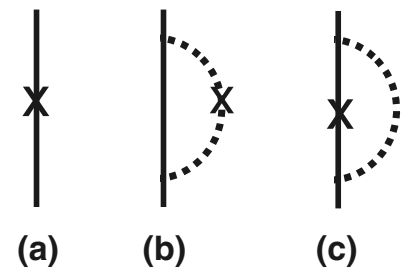


FIG. 2. (a) External interaction, X, with bare nucleon (solid line). (b) External interaction, X, with the pion. (c) External interaction, X, with the intermediate baryon. Here X represents the deep-inelastic-scattering operator.

The evaluation proceeds as for the intermediate nucleon. The result is

$$f_{\pi\Delta}(y) = \frac{1}{12\pi^2}\left(\frac{g_{\pi N\Delta}}{2M}\right)^2 y\int_{t_\Delta}^\infty dt\,\frac{F_A^2(t)}{(t+\mu^2)^2}$$
$$\times\left[t + \frac{1}{4M_\Delta^2}\left(M^2 - M_\Delta^2 + t\right)^2\right][(M+M_\Delta)^2 + t], \tag{12}$$

with $t_\Delta = [y^2M^2 + y(M_\Delta^2 - M^2)]/(1-y)$.

The previous material completes the discussion of the formalism.

## III. APPLICATION TO PARTON DISTRIBUTIONS

The next step is to use Eq. (3) to compute the light-flavor sea of a nucleon. Consider the role of the pion cloud in deep-inelastic scattering (Fig. 2). One needs to include terms in which the virtual photon hits (a) the bare nucleon, (b) the intermediate pion [44], and (c) the intermediate baryon $B$ of the $(\pi B)$ Fock-state component.

The effects of the Weinberg-Tomazowa (WT) term vanish because the deep-inelastic-scattering (DIS) operator, represented by X in the figure, is diagonal in the pion flavor index. Deep-inelastic scattering is a form of virtual Compton scattering. This scattering operator only takes a pion of a given charge into a pion of the same charge. This operator cannot change a flavor index so there is no effect. In more detail, denoting the DIS operator as $\mathcal{M}_{bb}$, the evaluation of the WT looks schematically like $\tau^a\epsilon^{abc}\pi^b\partial_\mu\pi^b\mathcal{M}_{bb} = 0$. Of course, the electromagnetic interaction, which explicitly depends on the charge of the pion and is off-diagonal in the flavor indices, does yield a contribution, as has been known for a long time; see e.g., Ref. [20]. However, any implication that the WT term leads to a contribution to DIS is simply wrong.

Another key assumption of the present model is that quantum interference effects involving different Fock-space components are negligible because different final states obtained from deep-inelastic scattering by the pion and by the nucleon are expected to be orthogonal.

Given the lack of interference effects, one can represent the quark distribution functions of flavor $f = (\bar{u}, \bar{d})$ in the nucleon sea as

$$q_N^f(x) = Zq_{N0}^f(x) + \sum_{B=N,\Delta} f_{\pi B}\otimes q_\pi^f + \sum_B f_{B\pi}\otimes q_B^f, \tag{13}$$

in which $f_{\pi B} \otimes q_\pi^f \equiv \int_x^1 \frac{dy}{y} f_{\pi B}(y) q_\pi^f(\frac{x}{y})$. The first symbol in the subscript represents the struck hadron, and the phase-space factor in Eq. (3) ensures that $f_{\pi B}(y) = f_{B\pi}(1-y)$. The quark distributions of the hadrons in the cloud are given by $q_\pi^f(x)$ and $q_B^f(x)$, and the bare nucleon distributions are given by $q_{N0}^f(x)$. We assume that the $\bar{u}, \bar{d}$ parton distributions of the bare proton and the intermediate $\Delta$ and nucleon are the same, $q_{N0}^f = q_\Delta^f = q_B^f$, and are flavor symmetric, as expected from the perturbative generation of sea quarks via the flavor-independent quark-gluon coupling constant.

Our Fock-space expansion has no one-to-one correspondence with Feynman diagrams. For example, the Feynman diagram of Fig. 2(b) would involve transitions from two-pion states to zero-pion states. Such effects should not be included because the light-cone Fock-space wave function is used to obtain probability distributions.

Contributions to the antiquark sea of the proton come from the valence and sea distributions of the pion, $q_\pi^v$ and $q_\pi^s$, and the sea distributions $q_B^s$ and $q_N^s$ of the intermediate baryons and the bare proton. The use of these distributions to describe deep-inelastic scattering from a bound pion follows from the light-front Fock-space expansion (3), which involves only on-mass-shell constituents. With $f_{\pi^+ n} = \frac{2}{3} f_{\pi N}$, $f_{\pi^0 p} = \frac{1}{3} f_{\pi N}$, $f_{\pi^- \Delta^{++}} = \frac{1}{2} f_{\pi\Delta}$, $f_{\pi^0 \Delta^+} = \frac{1}{3} f_{\pi\Delta}$, $f_{\pi^+ \Delta^0} = \frac{1}{6} f_{\pi\Delta}$, the antiquark distributions are

$$\bar{d}(x) = \left(\frac{5}{6} f_{\pi N} + \frac{1}{3} f_{\pi\Delta}\right) \otimes q_\pi^v + \bar{q}_{\rm sym}(x), \tag{14}$$

$$\bar{u}(x) = \left(\frac{1}{6} f_{\pi N} + \frac{2}{3} f_{\pi\Delta}\right) \otimes q_\pi^v + \bar{q}_{\rm sym}(x), \tag{15}$$

where $\bar{q}_{\rm sym}(x) \equiv \sum_B f_{\pi B} \otimes q_\pi^s + \sum_B f_{B\pi} \otimes q_B^s + Z q_N^s(x)$. The $\pi N$ terms favor the $\bar{d}$, but the $\pi\Delta$ terms favor the $\bar{u}$.

The pion valence quark parton distribution function (pdf) is obtained by evolving the pion valence pdfs of Aicher, Schäfer, and Vogelsang (ASV) [45] from their starting scale to $Q^2 = 54$ GeV$^2$, which is the scale relevant for E866. The present fit to the evolved valence distribution is given by $q_\pi^v(x) = 1.39\, x^{-0.331}(1-x)^{3.12}(7.18\, x^2 + 1)$. As in the ASV analysis, the pion sea quark pdfs are those of Gluck, Reya, and Schienbein [46], for which at 54 GeV$^2$, $q_\pi^s(x) = 0.115\, x^{-1.21}(1-x)^{5.34}(1 - 2.38\sqrt{x} + 4.28\, x)$.

Holtmann *et al.* [14] explained that the bare proton sea cannot directly be determined from experimental data, which includes contributions from the pion cloud. They ultimately [47] used a fit to DIS data that included corrections for the pion cloud to determine the bare proton sea. We use their symmetric sea: $x q_{N0}^{\bar{d}}(x) = x q_{N0}^{\bar{u}}(x) = 0.217(1-x)^{15.6}(1 + 0.625x)$. This distribution is also used for terms of Fig. 2(c).

Other input parameters must be described before presenting numerical results. The pion-nucleon splitting function $f_{\pi N}(y)$ depends on the coupling constant $g_{\pi N}$ and the form factor cutoff $\Lambda$. The lower limit for $g_{\pi N}$ is 12.8, taken from the Goldberger-Treiman relation $g_{\pi N} = \frac{M}{f_\pi} g_A$, with $g_A = 1.267 \pm 0.04$, $M = 0.939$ GeV, $f_\pi = 92.6$ MeV. The upper limit is $g_{\pi N} = 13.2$, consistent with the scattering data analysis of Perez *et al.* [48] and the muon-based determination of $g_A$ by Hill *et al.* [49]. As noted above, the cutoff parameter of

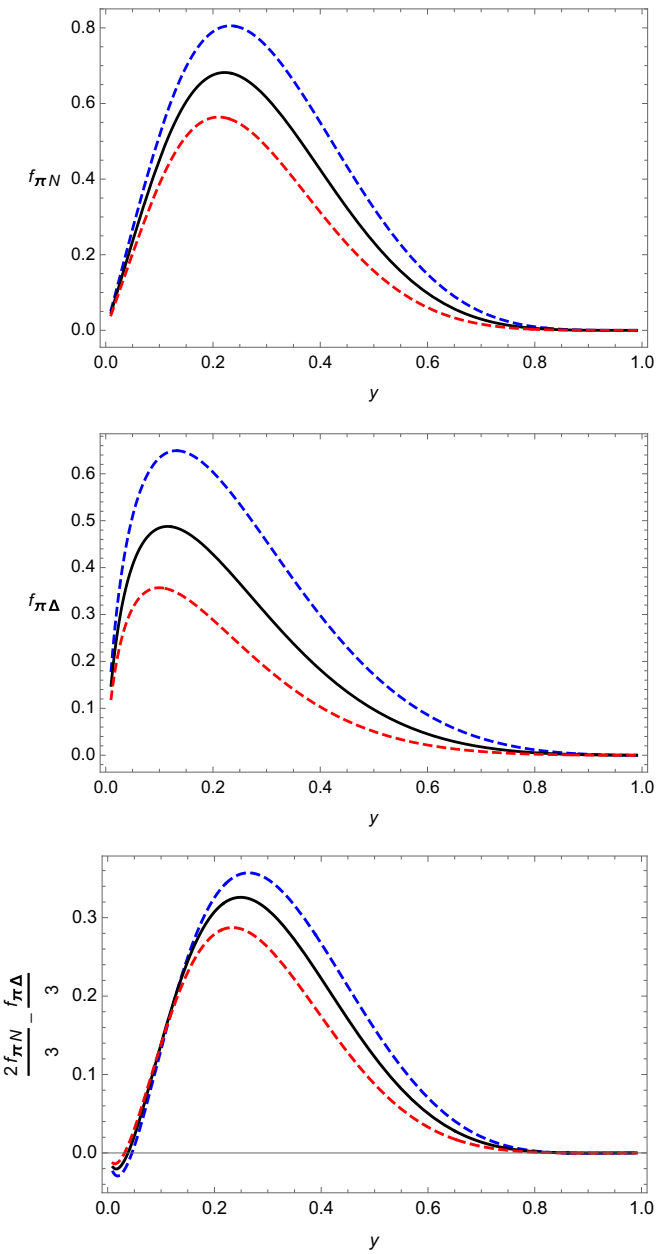


FIG. 3. Pion-baryon splitting functions $f_{\pi B}(y)$, $B = N, \Delta$, are shown in the upper two panels. The solid lines are found by using the central values of our coupling constants and cutoffs. The upper (blue) and lower (red) dashed lines are obtained by using the maximum or minimum values, respectively, of these parameters. The lowest panel shows the contribution of the splitting functions to the integrated asymmetry, $\bar{D} - \bar{U}$, Eq. (16). The smaller spread between the dashed lines is due to the correlation between the coupling constants and the use of the same cutoff in $f_{\pi N}(y)$ and $f_{\pi\Delta}(y)$.

Eq. (8), $\Lambda = \sqrt{3}/2M_A$, is obtained at very low $t$. The two resulting splitting functions are identical for all values of $y$, demonstrating that only small values of $t$ are important in the present calculations. In initial calculations we used the value $M_A = 1.03 \pm 0.04$ GeV [38]. This early review result was confirmed by many authors [50–54], all obtaining results within the stated uncertainty. We have increased the

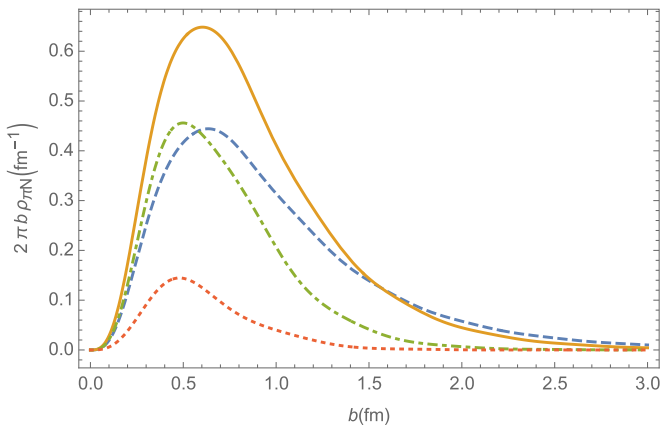


FIG. 4. $2\pi b\,\rho_{\pi N}(y,b)$ for $y = 0.1$ (dashed), 0.2 (solid), 0.4 (dot-dashed), and 0.6 (dotted), using the central values of our parameters for $f_{\pi N}(y)$.

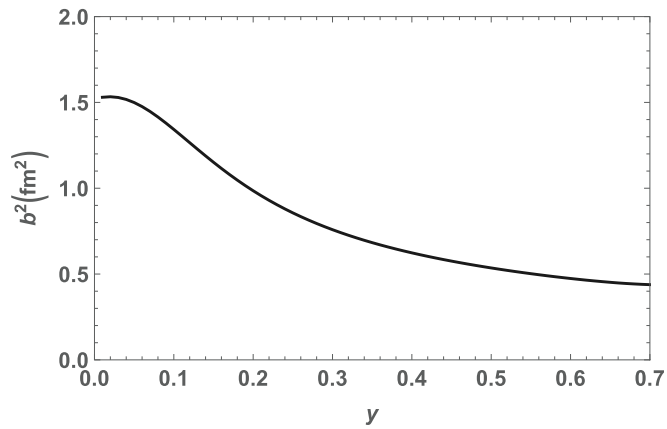


FIG. 5. $\langle b^2(y)\rangle$ for $\rho_{\pi N}(y,b)$ using the central values of our parameters for $f_{\pi N}(y)$.

uncertainty in our cutoff $\Lambda$ to $\pm 10\%$ to allow for a difference between the cutoffs in the $\pi NN$ form factor and the axial form factor. Although one early estimate, based on the cloudy bag model, suggested that the difference might be $\pm 20\%$ [39], later work using dispersion relations found consistency between the axial form factor cutoff and a $\pi NN$ *monopole* cutoff of $\Lambda = 0.80$ GeV $\pm 10\%$ [55,56]. A monopole value of $\Lambda = 0.8$ GeV corresponds to a dipole value of 1.1 GeV.

## IV. NUMERICAL RESULTS

The splitting function $f_{\pi N}(y)$ is shown in Fig. 3 for a range of parameters bounded by the maximum and minimum values of $g_{\pi N}$ and $\Lambda$. The splitting function $f_{\pi\Delta}(y)$ depends on the coupling constant $g_{\pi\Delta}$ and the form factor cutoff $\Lambda$. We use the same form factor and cutoff for $f_{\pi N}(y)$ and $f_{\pi\Delta}(y)$. The upper limit of the coupling constant is obtained by using the quark-model result $(\frac{g_{\pi\Delta}}{g_{\pi N}})^2 = \frac{72}{25}$, $g_{\pi\Delta} = 1.7 g_{\pi N}$. The lower limit of the coupling constant is obtained from the large-$N_C$ limit of $g_{\pi\Delta} = 1.5\, g_{\pi N}$. The ratio $f_{\pi\Delta}(y)/f_{\pi N}(y)$ is less than unity for the important regions of $y$. It does increase as $y$ increases above 0.5 and becomes greater than unity at about $y = 0.8$, where both splitting functions are vanishingly small.

The next step is to show that the splitting functions arise from the long-range structure of the nucleon. Figure 4 displays the transverse probability distribution $2\pi b\rho_{\pi N}(y,b)$ for several values of $y$, the momentum fraction carried by the pion. Central values of the parameters are used. Examination shows that the distribution is greatest for $y \approx 0.2$ and all distributions peak at a transverse distance $b \approx 0.6$ fm. This is a larger value than the 0.5 fm shown in Fig. 3 of Ref. [16]. This greater distance is caused by the use of our soft form-factors. Furthermore, Fig. 5 displays the mean-square value of $b$. This distribution peaks at small $y$, in the region in which chiral contributions are expected to be made [16], but there are long-ranged contributions to the $\pi N$ transverse probability for all values of $y$. Strikman and Weiss [16] note that, for small values of $b$, the transverse distribution of pions in the nucleon is strongly dependent on form factors and cutoffs and so argue that the pion-cloud contribution can only be safely determined for large $b \geqslant 0.5$ fm. Our calculation using the experimentally constrained soft vertex functions shows that the pionic effects are of long range (greater than at least 1 fm) for all values of $y$. This means that it is not necessary to eliminate all contributions below 0.5 fm. This unnecessary constraint used in Ref. [16] led to their Fig. 7, showing that the pion-cloud effect accounts for only for about half of the observed asymmetry. Furthermore the long-ranged nature of the contributions verify that large values of $t$ are not important in these calculations.

Finally, it has been known for a long time that the use of soft form factors (similar in range to those of the present study) leads to a convergent perturbation series [9–11,57,58]. Thus the present perturbative procedure is justified.

Having justified the model, let us turn to the observations. The integrated asymmetry $\bar{D} - \bar{U}$ is the difference in number of $\bar{d}$ and $\bar{u}$ quarks in the proton sea. With $\bar{D} = \int_0^1 \bar{d}(x)dx$, $\bar{U} = \int_0^1 \bar{u}(x)dx$, the asymmetry is determined from Eqs. (14) and (15) as

$$\bar{D} - \bar{U} = \frac{2}{3}\int_0^1 dy f_{\pi N}(y) - \frac{1}{3}\int_0^1 dy f_{\pi\Delta}(y). \qquad (16)$$

The experiment E866 [5] measured $\bar{D} - \bar{U} = 0.118 \pm 0.012$. Our splitting functions predict $0.98 \leqslant \bar{D} - \bar{U} \leqslant 0.131$, in excellent agreement with the experimental result.

The computed values of $\bar{d}(x) - \bar{u}(x)$ are compared with measurements in Fig. 6, with bands obtained by using minimum and maximum values of the splitting functions shown in Fig. 3. The upper band is for $p \to \pi N$, the lower is for $p \to \pi\Delta$. The central band shows the sum of these two contributions. Its width is narrow because of the correlation between the coupling constants: $g_{\pi\Delta} = r g_{\pi N}$, with $1.5 \leqslant r \leqslant 1.7$, and the use of the same cutoff $\Lambda$ for both terms. The central band is a definitive prediction of the present model. We stress that in *any* model, $\bar{u}$ and $\bar{d}$ are correlated so that errors in each are partially canceled in the ratio. We find that a 15% uncertainty in $\bar{d}$, $\bar{u}$ at $x = 0.3$ translates to 7% in the ratio.

The calculations of the ratio $\bar{d}(x)/\bar{u}(x)$ are compared with experimental data in Fig. 7. The results for values of $x$ less than about 0.15 arise from a combination of pion-cloud effects

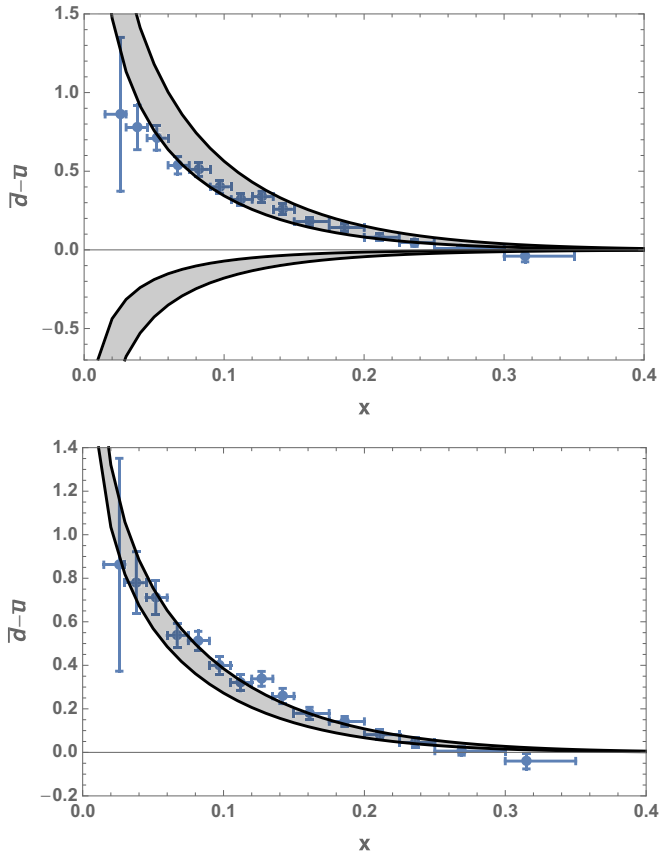


FIG. 6. $\bar{d}(x) - \bar{u}(x)$. Blue symbols are E866 data [5]. The bands are computed by using minimum and maximum values of the splitting functions shown in Fig. 3. In the top panel, the upper band is for $p \to \pi N$, the lower band is for $p \to \pi\Delta$. In the lower panel, the band represents the sum of the two contributions.

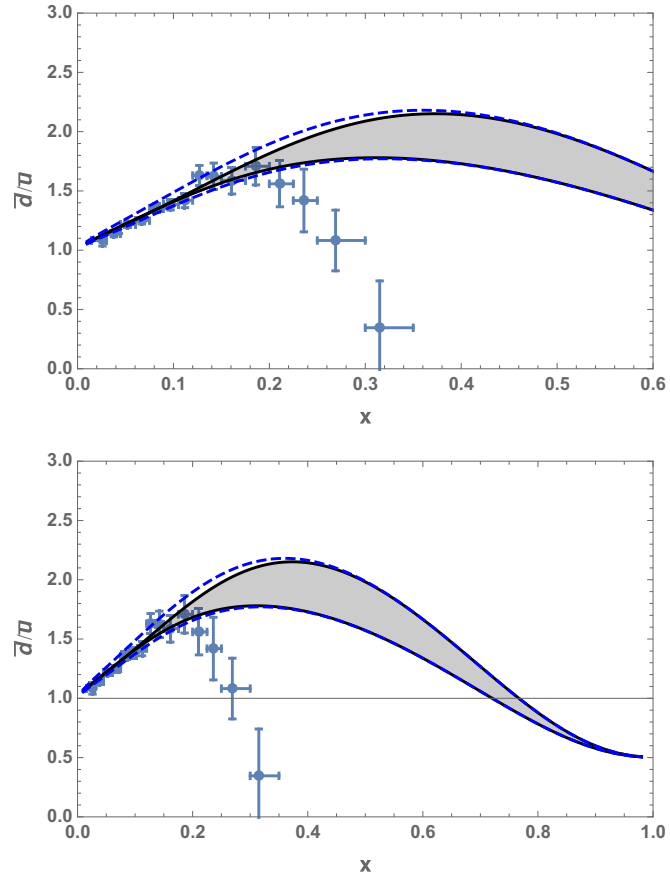


FIG. 7. $\bar{d}(x)/\bar{u}(x)$ Blue symbols are E866 data [5]. In the upper panel, the domain of the plot includes the range of $x$ covered in the SeaQuest experiment [6]. The solid band is computed by using minimum and maximum values of the splitting functions shown in Fig. 3, using the bare sea of Ref. [47]. The dashed band includes the effects of varying the bare sea by a factor of 0.75 or 1.25. The dashed band represents our prediction for the results of the SeaQuest experiment. In the lower panel, the domain of the plot is extended to $x = 1$.

and the symmetric sea of the bare nucleon. For larger values of $x$, terms of Fig. 2(b) dominate, with the $\pi N$ contribution rising with increasing $x$ until $x \approx 0.4$. The ratio then drops because of the enhancement of $\bar{u}$ [Eq. (15)] provided by the $\pi\Delta$ contribution, which becomes relatively more important as $x$ increases.

Excellent agreement with experimental data is obtained for $x < 0.2$, but the decrease in the ratio $\bar{d}(x)/\bar{u}(x)$ for higher values of $x$ is not reproduced. This disagreement might seem to rule out this model calculation. However, E866 is the only data set that impacts this quantity, and it is therefore important to determine if this behavior is correct. The displayed band predicts the results of the SeaQuest experiment, which will cover the range $0.1 \leqslant x \leqslant 0.6$ and this should definitively resolve these questions.

A point of interest in previous literature, due to the dramatic turn-down of the data (Fig. 7), is the limit as $x \to 1$. For large values of $x$ the pion valence quark distributions dominate, although both $\bar{u}(x)$ and $\bar{d}(x)$ become vanishingly small. The ratio

$$\frac{\bar{d}(x)}{\bar{u}(x)} \approx \frac{\left(\frac{5}{6}f_{\pi N} + \frac{1}{3}f_{\pi\Delta}\right) \otimes q_\pi^v}{\left(\frac{1}{6}f_{\pi N} + \frac{2}{3}f_{\pi\Delta}\right) \otimes q_\pi^v} \tag{17}$$

does not vanish, and $\bar{d}(x)/\bar{u}(x)$ approaches $1/2$ because of the explained greater importance of the $\pi\Delta$ term for $x \to 1$. This shows one mechanism that allows $\bar{d}/\bar{u}$ to drop below unity, but it is not likely that experiments will ever reach such values of $x$.

Some readers may be concerned that this model's form factors produce a flavor-singlet sea $x(\bar{u} + \bar{d})$ in excess of what is allowed by empirical parton densities that account for QCD evolution. That this is not the case is shown in Fig. 8, which compares $x(\bar{u} + \bar{d})$ for the present model to the NLO CT14 calculation. The resulting distributions are seen to be well below what is allowed. The contribution of the bare sea (included in the plot of the total flavor-singlet sea), determined at $Q^2 = 4$ GeV$^2$, is also much smaller than the CT14 distribution. The effects of QCD evolution of the bare sea from $Q^2 = 4$ GeV$^2$ to $Q^2 = 54$ GeV$^2$ are to decrease the bare sea for $x > 0.14$ and increase it for $x < 0.14$ [59]. These changes are smaller than the uncertainty bands that we used for the bare sea, and much less than the difference between CT14 (dashed line) and our calculation (solid line).

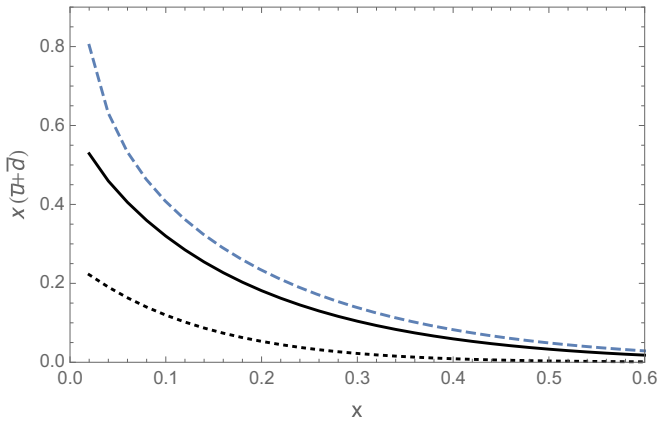


FIG. 8. The flavor-singlet sea $x(\bar{u}+\bar{d})$ of this model (solid line) compared with the next-to-leading order CT14 calculation (dashed line) for $Q^2 = 54$ GeV$^2$. The dotted line is the contribution of the bare sea to our model calculation. Central values of the distributions are used for all curves.

Therefore, our total sea does not exceed the bounds set by CT14.

## V. SUMMARY

The pion-baryon form factors of this model are essentially model independent, and the coupling constants are reasonably well determined. For values of $x$ greater than about 0.15, the pion-cloud effects dominate. The rise and then fall of the ratio $\bar{d}/\bar{u}$ are unalterable consequences of our approach. Significantly changing any of the input parameters would cause severe disagreements with other areas of nuclear physics and would be tantamount to changing the model. If the high-$x$ E866 results were to be confirmed by the SeaQuest experiment, the model would be ruled out.

In summary, this work presents a chiral light-front perturbation theory calculation of the wave function that describes the flavor content of the nucleonic light-quark sea. The formalism shows how to properly obtain vertex functions in a four-dimensional treatment. This allows us to obtain results which include the effects of the uncertainties in the input parameters, small enough to provide a definitive test of the pion cloud's role in the nucleon sea. The pion-cloud influence in the nucleon sea will be ruled out if our results were to disagree with the eventual results of the SeaQuest experiment.

## ACKNOWLEDGMENTS

The work of M.A. was supported by the Research in Undergraduate Institutions Program of the US National Science Foundation under Grant No. 1516105. The work of G.A.M. was supported by the USDOE Office of Science, Office of Nuclear Physics under Grant No. DE-FG02-97ER-41014. Support by MIT's Laboratory for Nuclear Science, USDOE Office of Science, Office of Nuclear Physics under Grant No. DE-FG02-94ER40818 is also gratefully acknowledged by G.A.M.

[1] P. Amaudruz *et al.* (New Muon Collaboration), The Gottfried Sum from the Ratio $F_2^n/F_2^p$, Phys. Rev. Lett. **66**, 2712 (1991).
[2] A. W. Thomas, A limit on the pionic component of the nucleon through SU(3) flavor breaking in the sea, Phys. Lett. B **126**, 97 (1983).
[3] E. M. Henley and G. A. Miller, Excess of anti-D over anti-U in the proton sea quark distribution, Phys. Lett. B **251**, 453 (1990).
[4] E. A. Hawker *et al.* (NuSea Collaboration), Measurement of the Light Anti-Quark Flavor Asymmetry in the Nucleon Sea, Phys. Rev. Lett. **80**, 3715 (1998).
[5] R. S. Towell *et al.* (NuSea Collaboration), Improved measurement of the $\bar{d}/\bar{u}$ asymmetry in the nucleon sea, Phys. Rev. D **64**, 052002 (2001).
[6] C. A. Aidala *et al.* (SeaQuest Collaboration), The SeaQuest spectrometer at Fermilab, arXiv:1706.09990v2 [physics.ins-det].
[7] J. Speth and A. W. Thomas, Mesonic contributions to the spin and flavor structure of the nucleon, Adv. Nucl. Phys. **24**, 83 (1997).
[8] W. C. Chang and J. C. Peng, Flavor structure of the nucleon sea, Prog. Part. Nucl. Phys. **79**, 95 (2014).
[9] S. Théberge, A. W. Thomas, and G. A. Miller, Pionic corrections to the MIT bag model: The (3,3) resonance, Phys. Rev. D **22**, 2838 (1980); **23**, 2106(E) (1981).
[10] A. W. Thomas, S. Théberge, and G. A. Miller, The cloudy bag model of the nucleon, Phys. Rev. D **24**, 216 (1981).
[11] S. Théberge, G. A. Miller, and A. W. Thomas, The cloudy bag model. 4. Higher-order corrections to the nucleon properties, Can. J. Phys. **60**, 59 (1982).
[12] V. Bernard, N. Kaiser, J. Kambor, and U. G. Meißner, Chiral structure of the nucleon, Nucl. Phys. B **388**, 315 (1992).
[13] V. Bernard, N. Kaiser, and U. G. Meißner, Chiral dynamics in nucleons and nuclei, Int. J. Mod. Phys. E **4**, 193 (1995).
[14] H. Holtmann, A. Szczurek, and J. Speth, Flavor and spin of the proton and the meson cloud, Nucl. Phys. A **596**, 631 (1996).
[15] W. Koepf, L. L. Frankfurt, and M. Strikman, The nucleon's virtual meson cloud and deep inelastic lepton scattering, Phys. Rev. D **53**, 2586 (1996).
[16] M. Strikman and C. Weiss, Chiral dynamics and partonic structure at large transverse distances, Phys. Rev. D **80**, 114029 (2009).
[17] M. Strikman and C. Weiss, Quantifying the nucleon's pion cloud with transverse charge densities, Phys. Rev. C **82**, 042201(R) (2010).
[18] M. Alberg and G. A. Miller, Taming the Pion Cloud of the Nucleon, Phys. Rev. Lett. **108**, 172001 (2012).
[19] C. R. Ji, W. Melnitchouk, and A. W. Thomas, Equivalence of pion loops in equal-time and light-front dynamics, Phys. Rev. D **80**, 054018 (2009).
[20] M. Burkardt, K. S. Hendricks, C. R. Ji, W. Melnitchouk, and A. W. Thomas, Pion momentum distributions in the nucleon in chiral effective theory, Phys. Rev. D **87**, 056009 (2013).
[21] C. R. Ji, W. Melnitchouk, and A. W. Thomas, Anatomy of

relativistic pion loop corrections to the electromagnetic nucleon coupling, Phys. Rev. D **88**, 076005 (2013).

[22] Y. Salamu, C. R. Ji, W. Melnitchouk, and P. Wang, $\bar{d} - \bar{u}$ Asymmetry in the Proton in Chiral Effective Theory, Phys. Rev. Lett. **114**, 122001 (2015).

[23] C. Granados and C. Weiss, Light-front representation of chiral dynamics in peripheral transverse densities, J. High Energy Phys. 07 (2015) 170.

[24] C. Granados and C. Weiss, Light-front representation of chiral dynamics with $\Delta$ isobar and large-$N_c$ relations, J. High Energy Phys. 06 (2016) 075.

[25] G. P. Lepage and S. J. Brodsky, Exclusive processes in perturbative quantum chromodynamics, Phys. Rev. D **22**, 2157 (1980).

[26] S. J. Brodsky, H. C. Pauli, and S. S. Pinsky, Quantum chromodynamics and other field theories on the light cone, Phys. Rep. **301**, 299 (1998).

[27] S. J. Brodsky, D. S. Hwang, B. Q. Ma, and I. Schmidt, Light cone representation of the spin and orbital angular momentum of relativistic composite systems, Nucl. Phys. B **593**, 311 (2001).

[28] Y. V. Kovchegov and E. Levin, Quantum chromodynamics at high energy, Cambridge Monogr. Math. Phys. **33**, 7 (2012).

[29] T. Becher and H. Leutwyler, Baryon chiral perturbation theory in manifestly Lorentz invariant form, Eur. Phys. J. C **9**, 643 (1999).

[30] T. R. Hemmert, B. R. Holstein, and N. C. Mukhopadhyay, $NN$, $N\Delta$ couplings and the quark model, Phys. Rev. D **51**, 158 (1995); S.-L. Zhu and M. J. Ramsey-Musolf, The off-diagonal Goldberger-Treiman relation and its discrepancy, *ibid.* **66**, 076008 (2002).

[31] V. Pascalutsa, Quantization of an interacting spin-$\frac{3}{2}$ field and the $\Delta$ isobar, Phys. Rev. D **58**, 096002 (1998).

[32] M. A. Alberg, E. M. Henley, and G. A. Miller, Omega meson cloud and the proton's light anti-quark distribution, Phys. Lett. B **471**, 396 (2000).

[33] P. F. Bedaque and U. van Kolck, Effective field theory for few-nucleon systems, Annu. Rev. Nucl. Part. Sci. **52**, 339 (2002).

[34] R. Machleidt and D. R. Entem, Chiral effective field theory and nuclear forces, Phys. Rep. **503**, 1 (2011).

[35] R. Machleidt, Historical perspective and future prospects for nuclear interactions, Int. J. Mod. Phys. E **26**, 1730005 (2017).

[36] T. M. Yan, Quantum field theories in the infinite-momentum frame III. Quantization of coupled spin-one fields, Phys. Rev. D **7**, 1760 (1973).

[37] G. A. Miller, Light front treatment of nuclei: Formalism and simple applications, Phys. Rev. C **56**, 2789 (1997).

[38] A. W. Thomas and W. Weise, *The Structure of the Nucleon*, (Wiley-VCH, Berlin, 2001).

[39] P. A. M. Guichon, G. A. Miller, and A. W. Thomas, The axial form-factor of the nucleon and the pion-nucleon vertex function, Phys. Lett. B **124**, 109 (1983).

[40] J. Carbonell, B. Desplanques, V. A. Karmanov, and J. F. Mathiot, -Explicitly covariant light-front dynamics and relativistic few-body systems, Phys. Rep. **300**, 215 (1998).

[41] G. A. Miller and B. C. Tiburzi, The relation between equal-time and light-front wave functions, Phys. Rev. C **81**, 035201 (2010).

[42] M. Burkardt, Impact parameter space interpretation for generalized parton distributions, Int. J. Mod. Phys. A **18**, 173 (2003).

[43] C. Alexandrou, G. Koutsou, T. Leontiou, J. W. Negele, and A. Tsapalis, Axial nucleon and nucleon to $\Delta$ form factors and the Goldberger-Treiman relations from lattice QCD, Phys. Rev. D **76**, 094511 (2007); **80**, 099901(E) (2009).

[44] J. D. Sullivan, One-pion exchange and deep inelastic electron-nucleon scattering, Phys. Rev. D **5**, 1732 (1972).

[45] M. Aicher, A. Schafer, and W. Vogelsang, Soft-Gluon Resummation and the Valence Parton Distribution Function of the Pion, Phys. Rev. Lett. **105**, 252003 (2010); M. Aicher (private communication).

[46] M. Gluck, E. Reya, and I. Schienbein, Pionic parton distributions revisited, Eur. Phys. J. C **10**, 313 (1999).

[47] A. Szczurek, V. Uleshchenko, H. Holtmann, and J. Speth, Production of the $W$ bosons and $Z$ bosons in the nucleon-anti-nucleon collisions and the meson cloud in the nucleon, Nucl. Phys. A **624**, 495 (1997).

[48] R. N. Perez, J. E. Amaro, and E. Ruiz Arriola, Precise determination of charge-dependent pion-nucleon-nucleon coupling constants, Phys. Rev. C **95**, 064001 (2017).

[49] R. J. Hill, P. Kammel, W. J. Marciano, and A. Sirlin, Nucleon axial radius and muonic hydrogen, Rep. Prog. Phys. **81**, 096301 (2018).

[50] V. Bernard, L. Elouadrhiri, and U. G. Meißner, Axial structure of the nucleon: Topical review, J. Phys. G **28**, R1 (2002).

[51] C. Juszczak, Running NUWRO, Acta Phys. Polon. B **40**, 2507 (2009).

[52] T. Katori and M. Martini, Neutrino-nucleus cross sections for oscillation experiments, J. Phys. G **45**, 013001 (2018).

[53] S. X. Nakamura *et al.*, Towards a unified model of neutrino-nucleus reactions for neutrino oscillation experiments, Rep. Prog. Phys. **80**, 056301 (2017).

[54] A. S. Meyer, M. Betancourt, R. Gran, and R. J. Hill, Deuterium target data for precision neutrino-nucleus cross sections, Phys. Rev. D **93**, 113015 (2016).

[55] R. Bockmann, C. Hanhart, O. Krehl, S. Krewald, and J. Speth, $\pi$NN vertex function in a meson-theoretical model, Phys. Rev. C **60**, 055212 (1999).

[56] T. E. O. Ericson, B. Loiseau, and A. W. Thomas, Determination of the pion nucleon coupling constant and scattering lengths, Phys. Rev. C **66**, 014005 (2002).

[57] R. F. Alvarez-Estrada and A. W. Thomas, Further studies of convergence in the cloudy bag model, J. Phys. G: Nucl. Phys. **9**, 161 (1983).

[58] G. A. Crawford and G. A. Miller, Convergent self-energy in the cloudy bag model, Phys. Lett. B **132**, 173 (1983).

[59] M. Tanabashi *et al.* (Particle Data Group), Review of particle physics, Phys. Rev. D **98**, 030001 (2018).